

Photoluminescence and excitation spectroscopy in heavily doped *n*- and *p*-type silicon

J. Wagner

Max-Planck-Institut für Festkörperforschung, Heisenbergstrasse 1, D-7000 Stuttgart 80, Federal Republic of Germany

(Received 12 September 1983)

Low-temperature photoluminescence and excitation spectroscopy measurements on heavily doped (up to $4 \times 10^{20} \text{ cm}^{-3}$) *n*- and *p*-type silicon are reported. From the luminescence spectra values for the optical and the reduced band gap are deduced and compared with theoretical calculations. The shrinkage of the reduced band gap follows an $n^{1/3}$ law for carrier concentrations n above the critical Mott density. Both *n*- and *p*-type samples show an identical shift of the reduced gap, whereas the shift of the optical gap is different due to the different density-of-states masses for electrons and holes. From photoluminescence excitation spectra the position of the optical gap is determined independently. A good agreement of the data obtained by these selective absorption measurements with the results from conventional luminescence spectra is found.

I. INTRODUCTION

The physical properties of heavily doped silicon are of practical as well as basic interest. The effect of heavy doping on the electronic properties of a semiconductor can be described, as can be the band-tailing effect due to the random impurity distribution, in terms of a reduction of the band gap.¹ The gap shrinkage represents the self-energy of the interacting charge carriers. Values for this shrinkage have been derived from optical-absorption,²⁻⁴ photoluminescence⁵⁻⁸ (PL), and transport data.⁹ Comparing these results major discrepancies have been noted between absorption and PL,⁶ as well as absorption and transport data.¹⁰

Theoretical work has been performed to calculate the band-gap reduction^{11,12} as well as the shape and energy position of the luminescence spectra of heavily doped silicon.¹³ The state of the art for calculating the band-gap shrinkage is shown for example in Fig. 7 of Ref. 12. The scatter of the experimental data is too large to allow an informative comparison between theory and experiment.

PL experiments measure the carrier distribution within the conduction or valence band as well as the carrier-induced band-gap reduction via the radiative recombination of photoexcited minority carriers.^{6,8} In Fig. 1 the electronic transitions possible in a heavily doped *n*-type semiconductor are shown. The conduction band is filled up to the Fermi energy E_F and optical absorption only occurs when the photon energy is high enough to excite an electron from the top of the valence band to an empty state in the conduction band. The energy gap involved is called the optical gap $E_{G,1}$. For the emission of a photon, on the other hand, the initial state of the electron has to lie between the bottom of the conduction band and the Fermi level. Therefore the PL band extends from the optical-gap energy $E_{G,1}$ (high-energy cutoff) to the energy of the reduced gap $E_{G,2}$ (low-energy edge). Absorption and emission spectra of heavily doped materials are complementary in the sense that the first one monitors the empty states of the conduction band and the second one

monitors the filled states of the conduction band.

The line shape of this luminescence band, $I(h\nu)$ can be expressed in terms of the density of states $D(E)$ and of the Fermi distribution function $f(E)$,⁸

$$I(h\nu) \sim D(h\nu - E_{G,2}) f(h\nu - E_{G,2}). \quad (1)$$

In this expression the energy dependence of the electric-dipole matrix element is neglected. In addition the photo-created holes are assumed to be thermalized at the top of the valence band and their density has to be much smaller than the electron concentration. The considerations made above for *n*-type doping are also valid for *p*-type material

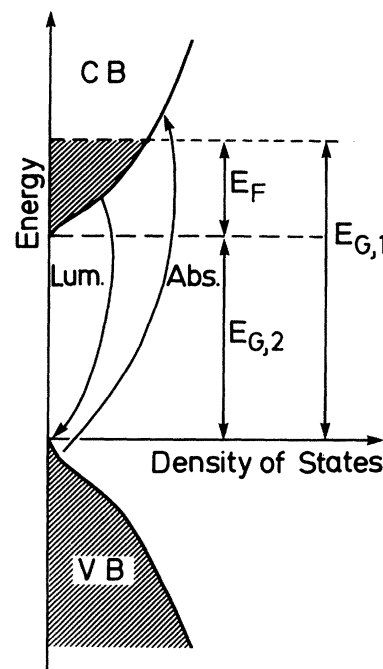


FIG. 1. Schematic drawing of the band structure of a heavily doped *n*-type semiconductor. Optical gap $E_{G,1}$ and reduced band gap $E_{G,2}$ as well as the band filling E_F are indicated.

by simply exchanging valence and conduction bands and electrons and holes, respectively.

In the PL spectrum of heavily doped silicon a second luminescence band besides the one discussed above can be observed, shifted to lower energies.⁵⁻⁷ As discussed by Parsons⁶ this band can be explained in terms of a recombination of majority carriers (electron or holes) with minority carriers (holes or electrons) bound to compensating impurities (acceptors or donors). These two luminescence bands show a different dependence on the exciting-laser power density. Low-excitation densities favor the low-energy band or so-called low-level (LL) luminescence, whereas high excitation is favorable for the band-to-band emission, the so-called high-level (HL) peak.^{5,7}

This study presents data obtained by PL and PL excitation (PLE) spectroscopy on heavily phosphorus- and boron-doped silicon samples. The doping level extends from 10^{17} cm^{-3} , which is well below the metal-insulator transition, up to 4×10^{20} cm^{-3} . The measurements have been carried out at 5 K. From the PL spectra the positions of the optical ($E_{G,1}$) and the reduced band gap ($E_{G,2}$) are obtained. The shift of the reduced band gap $E_{G,2}$ as a function of the carrier concentration n can be described by a $n^{1/3}$ power law. This shrinkage is the same for n - and p -type samples, whereas the shift of the optical gap is different. This is due to the difference in the density-of-states masses of electrons and holes in silicon. PLE spectroscopy has been used to measure the optical band gap in absorption on these heavily doped samples. This technique has the advantage of being only sensitive to band-to-band transitions, whereas conventional absorption measurements yield a superposition of band-to-band and free-carrier absorption. The data obtained for $E_{G,1}$ are in good agreement with the ones derived from the normal luminescence spectra, removing the discrepancy existing in the literature⁶ between the results of absorption and luminescence.

II. EXPERIMENT

The samples used in the present study were bulk-doped with phosphorus, arsenic, and boron. The impurity concentration extends from 10^{17} cm^{-3} up to 1.5×10^{20} cm^{-3} for phosphorus and 4×10^{20} cm^{-3} for boron. The arsenic-doped sample had an impurity concentration of 5×10^{19} cm^{-3} . The net impurity concentration was determined from room-temperature conductivity studies and checked by the measurement of the plasma frequency, which was obtained from the minimum in the infrared reflectivity. The surfaces of the samples were either polished or etched with a mixture of HF and HNO₃.

The samples were cooled by the exchange gas to 5 K. For the normal PL experiments they were excited by the 647-nm line of a Kr⁺ laser. For the excitation spectroscopy a tunable NaF:(F₂⁺)* color-center laser was used.^{14,15} The output power was 100–250 mW depending on the transparency of the output-coupling mirror. The laser could be tuned from 1.01 to 1.13 μm at a linewidth of 0.6 Å. A rather constant output power between 1.04 and 1.08 μm could be obtained by choosing the appropriate output-coupler reflectivity. The color-center laser was

optically pumped with a dye laser, emitting at 870 nm, which in turn was excited with the 647- and 676-nm lines of a Kr⁺ laser. The laser beam was focused to a spot size of about 500 μm on the silicon samples, resulting in an excitation density of 200–400 W/cm² for the 647-nm excitation. The luminescence was analyzed with a 1-m double monochromator and detected with an intrinsic Ge photodiode. A schematic drawing of the experimental set up is shown in Fig. 2.

III. RESULTS

A. Photoluminescence

Typical PL spectra are shown in Figs. 3 and 4 for various concentrations of phosphorus and boron. The PL spectra consist of three phonon replicas involving the momentum-conserving transverse-acoustic (TA) and transverse-optical (TO) phonons and the combination of the TO phonon and the optical zone-center phonon O^T, as can be seen clearly from the spectra with the lowest impurity concentration. For Si:P a strong no-phonon (NP) transition is also observed. With increasing impurity concentration the luminescence lines become broader, and for the most heavily doped samples only the TO and NP lines in the case of Si:P, and the TO and TA replicas for Si:B, can be distinguished. The temperature of 10 K indicated in the figures has been estimated from defect-induced luminescence spectra with known temperature dependence in other silicon samples excited under the same conditions as the samples under investigation here. It is higher than the temperature of the exchange gas due to the heating by the exciting-laser beam.

The spectra for phosphorus- as well as boron-doped silicon show pure high-excitation (HL) luminescence originating from band-to-band transitions as we checked by varying the excitation density. The high-energy edge of the NP luminescence line (for Si:P) or the TA replica (for Si:B) and the low-energy tail of the TO replica are indicat-

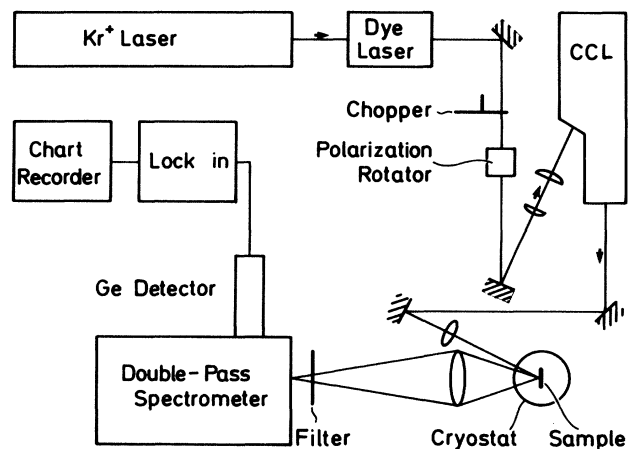


FIG. 2. Experimental setup for PLE spectroscopy using a tunable color-center laser. For conventional luminescence measurements the Kr⁺-laser beam was directly focused onto the sample.

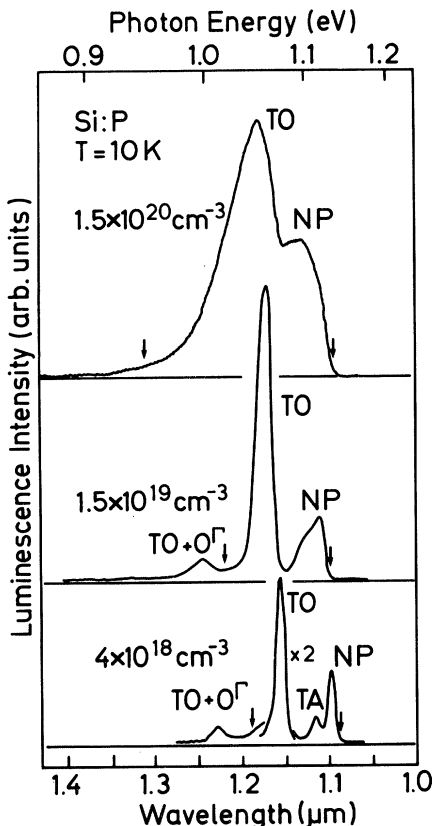


FIG. 3. PL of heavily doped Si:P for different donor concentrations. Arrows indicate the high-energy cutoff of the NP line $E_{G,1}$ and the low-energy edge of the TO replica $E_{G,2} - \hbar\omega_{TO}$. Spectral resolution was 8 Å for the lowest spectrum and 24 Å for the two upper spectra.

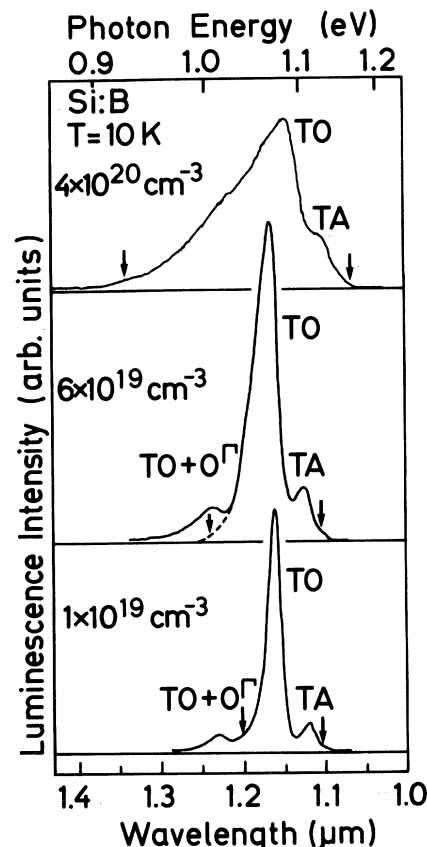


FIG. 4. PL of heavily doped Si:B for different acceptor concentrations. Arrows indicate the high-energy cutoff of the TA replica $E_{G,1} - \hbar\omega_{TA}$ and the low-energy edge of the TO replica $E_{G,2} - \hbar\omega_{TO}$. Spectral resolution was 8 Å for the lowest spectrum and 24 Å for the two upper spectra.

ed by arrows. The high-energy cutoff represents the optical gap $E_{G,1}$ and the low-energy edge represents the reduced band gap $E_{G,2}$ when taking into account the energies of the phonons involved in the recombination. The determination of $E_{G,1}$ is quite accurate due to the sharpness of the high-energy edge. In contrast, the low-energy tail of the TO replica is quite smooth. Hence the point at which the luminescence intensity is about 5% of the peak value has been taken to define the reduced band gap $E_{G,2}$.

Figures 5 and 6 display $E_{G,1}$ and $E_{G,2}$ as a function of the carrier concentration for n - and p -type material. The reduced band gap $E_{G,2}$ shifts to lower energies with increasing carrier concentration, whereas the optical gap $E_{G,1}$ remains either approximately constant for n -type samples or shows a slight shift to higher energies for p -type material. For n -type samples up to $4 \times 10^{19} \text{ cm}^{-3}$ the spectra found here are similar to those reported by Parsons *et al.*^{5,6} and Schmid *et al.*⁸ For higher dopant concentrations only one spectrum is shown in the literature,⁸ but as can be seen from the width of the HL luminescence band in this spectrum the carrier concentration has to be less than $1 \times 10^{20} \text{ cm}^{-3}$, the value quoted there.^{8,13} So there are no luminescence data available to compare with the present ones for electron concentrations above $4 \times 10^{19} \text{ cm}^{-3}$. For p -type material the spectra shown in the litera-

ture always contains contributions of both HL and LL luminescence^{7,8} which become strongly overlapping for high impurity concentrations. Therefore no informative comparison with the data presented here can be made.

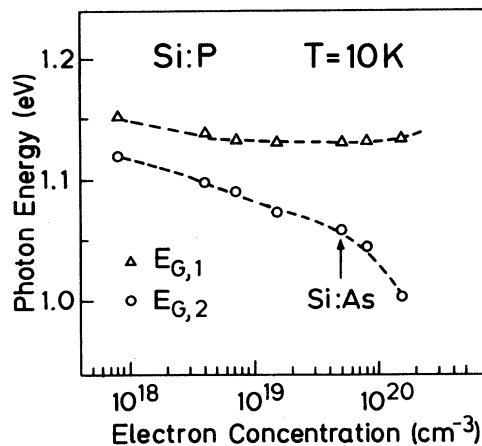


FIG. 5. Optical gap $E_{G,1}$ and reduced band gap $E_{G,2}$ vs carrier concentration for n -type silicon. Energies shown have been corrected for phonon energies involved.

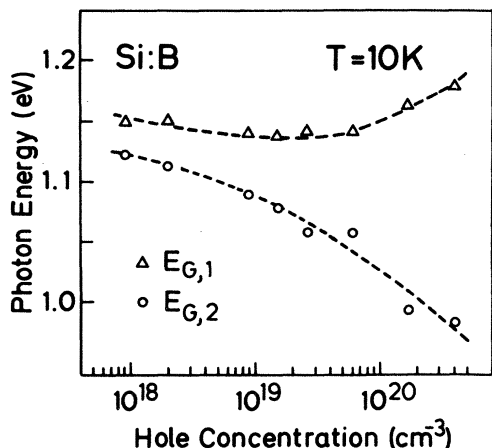


FIG. 6. Optical gap $E_{G,1}$ and reduced band gap $E_{G,2}$ vs carrier concentration for Si:B. Energies shown have been corrected for phonon energies involved.

B. Excitation spectroscopy

For excitations resonant with the indirect band gap in all samples except one, only the so-called LL luminescence has been observed. This is due to the low volume excitation density caused by the large penetration depth of the light. In Figs. 7 and 8 excitation spectra of the TO-phonon-assisted LL luminescence are shown for Si:P and Si:B together with an excitation spectrum of a "pure" sample. The electronic temperature in this case is very close to the bath temperature due to the small excess ener-

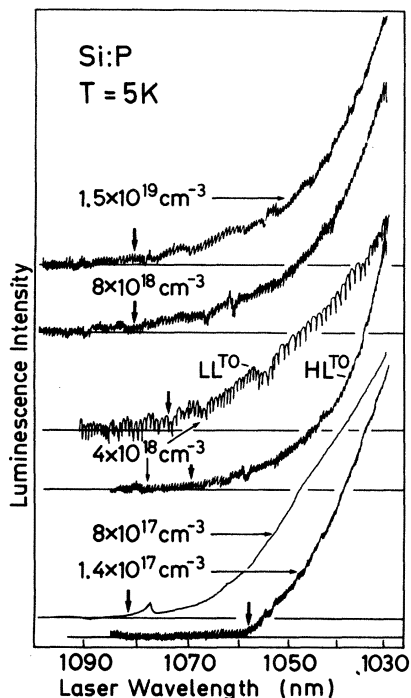


FIG. 7. PLE spectra of Si:P. Arrows indicate the position of the optical band gap. LL luminescence was used as the monitor transition for all spectra except the one specially indicated as HL^{TO}.

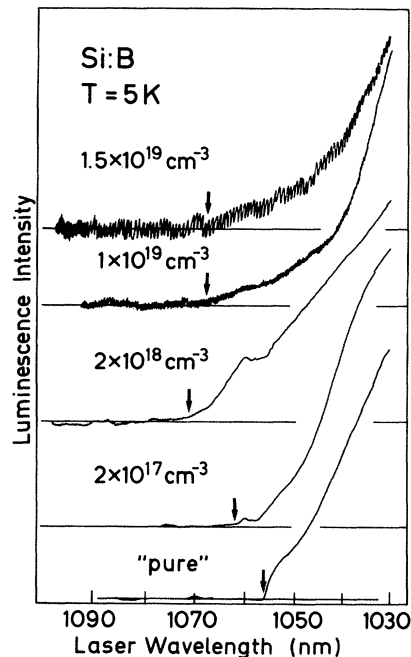


FIG. 8. PLE spectra of Si:B. Arrows indicate the position of the optical band gap. LL luminescence was used as the monitor transition for all spectra. Lowest trace shows for comparison an excitation spectrum of the free-exciton luminescence in a pure sample.

gy of the laser photons and the low excitation density.

For the pure sample with a net impurity concentration of $\approx 10^{13} \text{ cm}^{-3}$ both the free exciton as well as the bound exciton show the same excitation spectrum (lowest trace of Fig. 8). Comparing this spectrum with classical absorption data¹⁶ the steep onset at 1056.3 nm is identified with the onset of TA-phonon-assisted free-exciton absorption. For increasing impurity concentrations up to the critical Mott density of $3 \times 10^{18} \text{ cm}^{-3}$ a downwards shift of this TA-phonon-assisted absorption edge is observed for both *n*- and *p*-type samples. An additional structure appears at about 1060 nm in Si:B (2×10^{17} and $2 \times 10^{18} \text{ cm}^{-3}$) and at 1078 nm in Si:P ($8 \times 10^{17} \text{ cm}^{-3}$). For the $2 \times 10^{18} \text{ cm}^{-3}$ boron-doped sample this structure is more intense and broader than for the $2 \times 10^{17} \text{ cm}^{-3}$ doped sample. The spectral positions of these peaks in the excitation spectrum coincide with the high-energy edge of the HL emission in the normal luminescence spectra. Therefore they can be identified as absorption transitions involving the impurity band of boron or phosphorus, respectively. The feature in the PLE spectrum of Si:P is caused by an excitation without phonon participation of an electron out of the valence band into an empty state of the donor-related impurity band. The structure in the excitation spectra of Si:B is a similar transition of a hole to the acceptor impurity band with TA-phonon participation.

For impurity concentrations above the metal-insulator transition ($> 3 \times 10^{18} \text{ cm}^{-3}$) the PLE spectra show the onset of valence- to conduction-band absorption without any additional structure. For the $4 \times 10^{18} \text{ cm}^{-3}$ sample of

Si:P the luminescence spectrum exhibits both LL and HL emission even under resonant excitation. In Fig. 7 the PLE spectra of both HL and LL luminescence are displayed. The HL-excitation spectrum shows a steeper increase in absorption with increasing photon energy than the LL spectrum. This simply reflects the different dependence on excitation density of HL and LL luminescence. For exciting photon energies very close to the absorption edge the volume excitation density is very low, favoring LL emission. For increasing photon energies the penetration depth of the light becomes smaller, which increases the excitation density, and therefore enhances the HL luminescence.

The PLE spectra shown in Figs. 7 and 8 are not corrected for the spectral variation of the output power of the exciting laser. But, as mentioned in Sec. II, this variation was small. It does not affect the position of the absorption edge in the excitation spectra. This has been checked by comparison of the excitation and the conventional absorption spectrum of pure material. The optical gap $E_{G,1}$, which is defined by the onset of the band-to-band absorption, is marked by an arrow in Figs. 7 and 8. As can be seen from the PLE spectra of the 4×10^{18} -cm $^{-3}$ sample of Si:P this onset coincides, within a few meV, for the HL and LL spectra.

The values of $E_{G,1}$ determined from the PLE spectra, are shown in Fig. 9 for n - and p -type samples together with the position of the high-energy cutoff of the HL emission band in the normal luminescence spectra. All the data shown have been corrected for the energies of the phonons involved, so they represent electronic transition energies. For carrier concentrations below the Mott density the position of the high-energy edge of the luminescence remains constant, whereas the optical band gap as

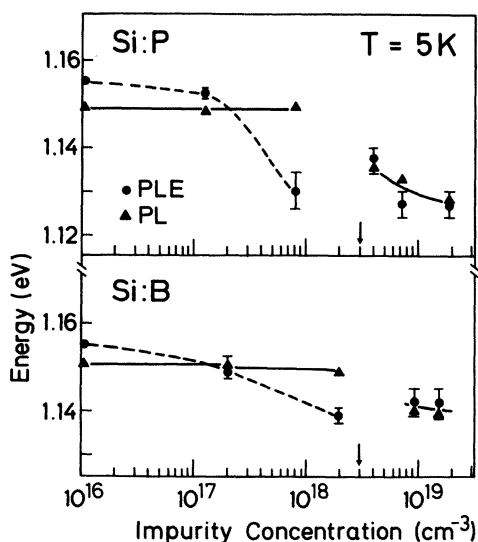


FIG. 9. Position of the optical band gap as determined by PLE and of the high-energy cutoff of the PL vs impurity concentration. All data shown have been corrected for the phonon energies involved. Critical Mott density is indicated by an arrow.

determined by PLE shows a shift to lower energies. For concentrations above $\approx 3 \times 10^{17}$ cm $^{-3}$ the PLE spectra give values for the gap, which are smaller than the highest photon energy seen in emission. For carrier concentrations exceeding $\approx 3-4 \times 10^{18}$ cm $^{-3}$ both PL and PLE spectra give, within the experimental error, identical results for $E_{G,1}$.

This agreement between absorption (PLE) data and luminescence results for doping level above the Mott density removes the discrepancy stated in the literature.^{6,13} Compared to the conventional absorption experiment the present technique of excitation spectroscopy or selective absorption gives much more accurate results because it is only sensitive to band-to-band transitions. Normal absorption, in contrast, monitors both band-to-band and intraband processes simultaneously, making it necessary to deconvolute the spectra obtained by fitting the free-carrier absorption at the long-wavelength part of the spectrum.⁴

The discontinuity of the PLE data for the optical gap at $\approx 3 \times 10^{18}$ cm $^{-3}$, the critical Mott density, will now be discussed. The excitation spectrum of the pure sample clearly shows TA-phonon-assisted excitonic absorption. For the samples with doping levels above 3×10^{18} cm $^{-3}$, on the other hand, no excitonic contributions are expected to occur because of screening effects. Despite the difficulty of distinguishing between valence- to conduction-band and valence- to impurity-band absorption for carrier concentrations of $10^{17}-10^{18}$ cm $^{-3}$, the tentative suggestion, that this discontinuity is caused by the breakdown of the excitonic binding at the Mott density, can be made. This tentative model is based on the assumption of an excitonic absorption edge in the above-mentioned doping range, in contrast to an impurity-band luminescence free of excitonic effects. The difference between the optical gap determined by PLE and the high-energy edge of the HL luminescence, amounting to 10–20 meV at $\approx 1 \times 10^{18}$ cm $^{-3}$, is comparable to the free-exciton binding energy of 14.7 meV,¹⁷ supporting the suggestion made above.

IV. DISCUSSION

In Fig. 10 and 11 the present results for the reduced band gap $E_{G,2}$ are displayed together with theoretical calculations by Berggren and Sernelius,¹² Mahan,¹¹ and Abram *et al.*¹ The experimental data for both n - and p -type material can be described by the following relation:

$$E_G(\text{pure}) - E_{G,2} \sim n^{1/3}, \quad (2)$$

with n as the charge carrier concentration.

For n -type doping the calculation by Berggren and Sernelius, assuming a random arrangement of the donor atoms, gives the best description of the experimental result. The band-gap reduction found experimentally is, however, somewhat larger than that predicted by this calculation. The calculation of Ref. 12, assuming a fcc arrangement of the impurities and the calculation by Mahan, in contrast, yields a much smaller band-gap reduction than found in the experiment. For p -type doping the only available theoretical calculation to compare with is the one by Abram *et al.*¹ Here again, the band-gap shrinkage as determined from the luminescence spectra is

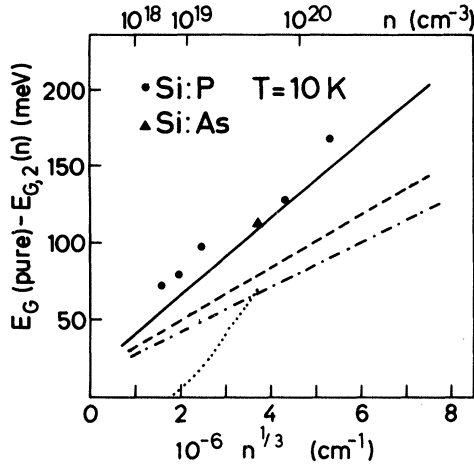


FIG. 10. Shift of the reduced band gap $E_G(\text{pure}) - E_{G,2}$ [$E_G(\text{pure}) = 1.17$ eV] vs carrier concentration n . Solid line refers to the calculation by Berggren and Sernelius (Ref. 12) assuming a random arrangement of the donors, and dashed line refers to the calculation assuming an arrangement in a fcc lattice. Dashed-dotted lines shows the result of Mahan's variational calculation (Ref. 11) and the dotted curve gives the results of absorption measurements by Schmid (Ref. 4).

somewhat larger than the theoretical prediction.

When comparing theory and experiment one has to keep in mind, for the calculations, any band-tailing effects have been neglected.^{1,11,12} The inclusion of band tailing results in a further reduction of the gap $E_{G,2}$.^{6,18} Following Benoit à la Guillaume and Cernogora¹⁸ this shift amounts to

$$\epsilon = \frac{\hbar^2}{2m_d} \left(\frac{4\pi n}{3} \right)^{2/3}, \quad (3)$$

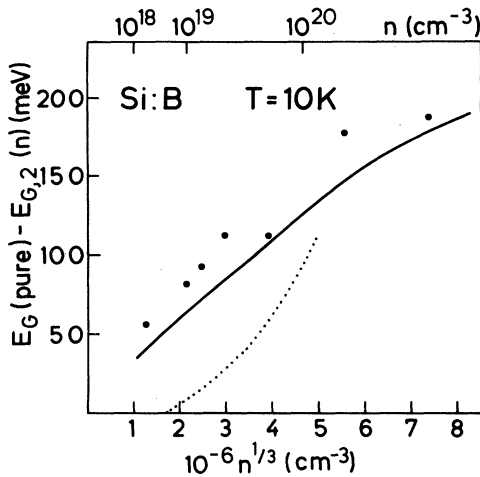


FIG. 11. Shift of the reduced band gap $E_G(\text{pure}) - E_{G,2}$ [$E_G(\text{pure}) = 1.17$ eV] vs carrier concentration n . Solid line shows the result of the Lindhard calculation by Abram *et al.* (Ref. 1) and the dotted curve refers to absorption data by Schmid (Ref. 4).

with m_d being the effective density-of-states mass of the minority carriers. Considering luminescence spectra taken at finite temperature the relevant quantity is $\bar{\epsilon}$, the energy of the maximum of the minority-carrier distribution.¹⁸ For electron concentrations of 10^{18} , 10^{19} , and 10^{20} cm^{-3} , one obtains $\epsilon \approx 1.7$, 8, and 37 meV, respectively. Assuming a carrier temperature of ≈ 10 K and nondegenerate holes,⁶ $\bar{\epsilon}$ amounts to ≈ 1.5 , 4, and 10 meV, respectively. So the effective reduction of the band gap $E_{G,2}$ due to band tailing is ≈ 0 , ≈ 4 , and ≈ 27 meV for 10^{18} , 10^{19} , and 10^{20} donors per cm^3 . Therefore the effect of band tailing becomes important only for the most heavily doped samples and it does not significantly alter the conclusions made above.

For p -type material this effect is reduced due to the larger density-of-states mass of the electrons. For an acceptor concentration of 10^{20} cm^{-3} the effective reduction amounts to only ≈ 13 meV compared to ≈ 27 meV for n -type doping.

The influence of the chemical nature of the donor or acceptor atom on the band-gap reduction has been calculated recently by Viña *et al.*¹⁹ They found a band-gap reduction which is 10% larger in Si:As than in Si:P for a donor concentration of 5×10^{20} cm^{-3} . In the experiment the band-gap reduction found for the arsenic-doped sample fits together with the data found for Si:P (see Fig. 10) indicating, at least, no strong dependence on the nature of the donor atoms. One has to keep in mind, however, that the influence of the nature of the impurity found in the above-mentioned calculations is comparable to the experimental accuracy. Therefore no definitive conclusion can be drawn on this point.

Also shown in Figs. 10 and 11 are the results of the absorption study by Schmid.⁴ He found the reduced band gap to vary with the carrier density as

$$E_G(\text{pure}) - E_{G,2} \sim \left(\frac{n - n_c}{n_c} \right)^\gamma, \quad (4)$$

with n_c a critical density of $5 - 6 \times 10^{18}$ cm^{-3} and $\gamma = 0.8$ as a critical exponent. The values obtained are much smaller than the ones found by luminescence. This discrepancy can possibly be explained by the rather complicated procedure needed to extract the gap position from the absorption data.⁴

The values of $E_{G,1}$ and $E_{G,2}$ obtained by PL as well as PLE measurements are displayed in Fig. 12 for carrier concentrations ranging from 10^{17} cm^{-3} to 4×10^{20} cm^{-3} . To the PLE data of $E_{G,1}$ for carrier concentrations below 3×10^{18} cm^{-3} the excitation binding energy of 14.7 meV (Ref. 17) has been added to remove the discontinuity of the optical gap at the critical Mott density (see Sec. III B). The reduced gap $E_{G,2}$ shows within the experimental error the same shrinkage for n - and p -type material. The optical gap, in contrast, behaves differently for donor or acceptor doping. For n -type samples it remains nearly constant from 4×10^{18} to 1.5×10^{20} cm^{-3} , whereas in p -type material an increase is observed for carrier concentrations above 10^{20} cm^{-3} . This difference in behavior is due to the difference in the effective density-of-states masses for electrons and holes. So the mass of the electrons,

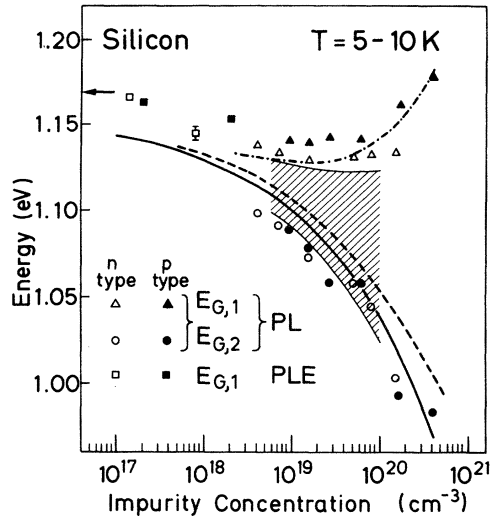


FIG. 12. Optical ($E_{G,1}$) and reduced band gap ($E_{G,2}$) as determined by PL and PLE spectroscopy vs carrier concentration for n - and p -type material. Arrow on the energy scale indicates the band-gap energy of pure silicon. Solid line shows the result of the calculation of $E_{G,2}$ in n -type material by Berggren and Sernelius (Ref. 12) and the dashed line refers to the calculation of $E_{G,2}$ for p -type doping by Abram *et al.* (Ref. 1). Hatched area indicates the width and position of the luminescence spectra calculated by Selloni and Pantelides (Ref. 13). Dashed-dotted line shows the optical gap for p -type silicon calculated using the results by Abram *et al.* and the carrier-concentration-dependent density-of-states masses for holes given by Barber (Ref. 22).

$m_{de} = 1.062m_0$, is nearly twice as large as the one of the holes, $m_{dh} = 0.577m_0$.^{20,21} In these quantities the sixfold degeneracy of the conduction band, as well as the degeneracy of the light and heavy valence band at the Brillouin-zone center, are included. The smaller mass of the holes results in a larger band filling in p -type material than in n -type samples for a given carrier concentration.

Figure 12 also displays theoretical curves for $E_{G,1}$ and $E_{G,2}$. For the reduced gap $E_{G,2}$ here, again the data by Berggren and Sernelius¹² and Abram *et al.*¹ are shown. For the low-density limit the theoretical curves approach the exciton binding energy, whereas the experimental data do not include any excitonic binding. Comparing the PL spectra calculated by Selloni and Pantelides¹³ with the experimental data presented here, a good agreement, espe-

cially for $E_{G,2}$, is found ($E_{G,1}$ and $E_{G,2}$ have been extracted from the calculated curves in the same way they were extracted from the experimental spectra). This agreement is remarkable because these calculations already include disorder effects. For the optical gap $E_{G,1}$ the data of Selloni and Pantelides are somewhat smaller, but this can be due to a higher carrier temperature in the experiment than that assumed for the calculation. In order to obtain theoretical data on the optical gap of p -type material, the Fermi energy was calculated using the density-dependent hole masses of Barber,²² and added to the calculated values for $E_{G,2}$.¹ The resulting curve reproduces the increase of the optical gap for doping levels above 10^{20} cm^{-3} found in the experiment.

The approximate constancy of the optical band gap $E_{G,1}$ for n -type material led Schmid *et al.*⁸ to conclude that the effective band-gap shrinkage $E_G(\text{pure}) - E_{G,2}$ goes as $n^{2/3}$ rather than $n^{1/3}$. The present results, however, clearly show that the gap shrinkage is proportional to $n^{1/3}$ for both n - and p -type samples. The constancy of $E_{G,1}$ for n -type doping in the concentration range ($6 \times 10^{18} - 1 \times 10^{20}$ cm^{-3}) under investigation in Ref. 8 is due to a rather flat minimum in the $E_{G,1}(n)$ relation at $\approx 5 \times 10^{19}$ cm^{-3} .

V. CONCLUSIONS

The variation of the optical band gap as well as the reduced gap with doping has been studied by PL and PLE spectroscopy. The values for the optical gap obtained by luminescence and selective absorption are in good agreement. The shrinkage of the reduced band gap is found to be proportional to the carrier concentration to the one-third ($n^{1/3}$). For both n - and p -type materials the same dependence of the reduced gap on the carrier concentration is observed, whereas the shift of the optical gap shows a different behavior due the differences in the density-of-states masses of electrons and holes. A detailed comparison of the experimental data presented here with calculations has been performed.

ACKNOWLEDGMENTS

I wish to thank Professor M. Cardona for many helpful and stimulating discussions, and H. Hirt, M. Siemers, and P. Wurster for valuable experimental assistance. Thanks are also due H. E. Schaefer, L. Raschke, and G. Steudle for the electron irradiation of the color-center-laser crystals.

¹R. A. Abram, G. J. Rees, and B. L. H. Wilson, *Adv. Phys.* **27**, 799 (1978).

²A. A. Vol'fson and V. K. Subashiev, *Fiz. Tekh. Poluprovodn.* **1**, 397 (1967) [*Sov. Phys.—Semicond.* **1**, 327 (1967)].

³M. Balkanski, A. Aziza, and E. Amzallag, *Phys. Status Solidi* **31**, 323 (1969).

⁴P. E. Schmid, *Phys. Rev. B* **23**, 5531 (1981).

⁵R. R. Parsons, *Can. J. Phys.* **56**, 814 (1978).

⁶R. R. Parsons, *Solid State Commun.* **29**, 763 (1979).

⁷R. R. Parsons, J. A. Rostworowski, and B. Bergersen, in *Proceedings of the 14th International Conference on the Physics of Semiconductors, Edinburgh, 1978*, edited by B. L. H. Wilson (Institute of Physics, London, 1979), p. 1267.

⁸P. E. Schmid, M. L. W. Thewalt, and W. P. Dumke, *Solid State Commun.* **38**, 1091 (1981).

⁹J. W. Slotboom and H. C. de Graaf, *Solid State Electron.* **19**, 857 (1976).

¹⁰R. W. Keyes, *Comments Solid State Phys.* **7**, 149 (1977).

- ¹¹G. D. Mahan, *J. Appl. Phys.* 51, 2634 (1980).
- ¹²K. F. Berggren and B. E. Sernelius, *Phys. Rev. B* 24, 1971 (1981).
- ¹³A. Selloni and S. T. Pantelides, *Phys. Rev. Lett.* 49, 586 (1982).
- ¹⁴L. F. Mollenauer, *Opt. Lett.* 5, 188 (1980).
- ¹⁵J. Wagner, J. Weber, and R. Sauer, *Solid State Commun.* 39, 1273 (1981).
- ¹⁶G. G. MacFarlane, T. P. McLean, J. E. Quarrington, and V. Roberts, *Phys. Rev.* 111, 1245 (1958).
- ¹⁷K. L. Shaklee and R. E. Nahory, *Phys. Rev. Lett.* 24, 942 (1970).
- ¹⁸C. Benoit à la Guillaume and J. Cernogora, *Phys. Status Solidi* 35, 599 (1968).
- ¹⁹L. Viña, P. B. Allen, and M. Cardona (unpublished).
- ²⁰G. Dresselhaus, A. F. Kiep, and C. Kittel, *Phys. Rev.* 98, 368 (1955).
- ²¹J. C. Hensel and G. Feher, *Phys. Rev.* 129, 1041 (1963).
- ²²H. D. Barber, *Solid State Electron.* 10, 1039 (1967).